Theor Chem Acc (2010) 126:87–98
DOI 10.1007/s00214-009-0685-y

REGULAR ARTICLE

Theoretical study of the competitive decomposition and isomerization of 1-hexyl radical

Feng Wang · Dong Bo Cao · Gang Liu · Jie Ren · Yong Wang Li

Received: 16 September 2009 / Accepted: 2 November 2009 / Published online: 24 November 2009

Abstract The ground-state potential energy surface of the 1-hexyl system, including the main decomposition and isomerization processes, has been calculated with the MPW1K, BB1K, MPWB1K, MPW1B95, BMK, M05-2X and CBS-QB3 methods. On the basis of these data, thermal rate coefficients of different reaction channels and branching ratios were then calculated using the master equation formulation at 250–2,500 K. The results clearly point out that the 1,5 H atom transfer reaction of 1-hexyl radical with exothermicity proceeds through the lowest reaction barrier, whereas the decomposition processes are thermodynamically unfavorable with large endothermicity. The temperature effect is important on the relative importance of different reactions in the 1-hexyl system. In the low-temperature range of 250–900 K, isomerization reactions, especially 1,5 H atom transfer reaction of 1-hexyl radical, are dominating and responsible for over 82.17% of all the reactions, due to their smaller reaction barriers than those of the decomposition reactions. Furthermore, an equilibrium process involving the isomeric forms of the hexyl radicals appearing at relative low temperature was validated theoretically. However, isomerization and decomposition processes are kinetically competitive and simultaneously important under normal pyrolysis conditions.

Keywords Density functional theory · Decomposition · Isomerization · 1-Hexyl radical · Rate coefficient

1 Introduction

Unimolecular decomposition and isomerization of alkyl radicals are an all-important part of the chemical schemes of many high-temperature processes such as hydrocarbon pyrolysis [1]. Furthermore, for long-chain alkyl radicals, the isomerization reactions are known to compete favorably with the direct decomposition processes [2]. The relative rates of these processes determine the role of the alkyl radicals in the ensemble of chain reactions, as the reactivity of the products of these reactions is different. Therefore, detailed knowledge of the kinetic behavior of such reactions is the key for accurately modeling these systems. However, very few of the experimental rate coefficients for these types of reactions have become known with a satisfactory accuracy. Especially, little is known about the microscopic features of related reactions of long-chain alkyl radicals with five carbons or more under normal pyrolysis conditions. This situation reflects the experimental difficulties of investigating the multi-channel reactions for these short-lived and highly reactive radicals. Quantum chemical methods can be used to calculate the important thermochemical properties and reaction rates of the complex reactions of alkyl radicals.

1-hexyl (1-C_6H_{13}) radical exhibits most of the important kinetic and mechanistic features, characteristic for the isomerization and decomposition of alkyl radicals with long carbon chains. It is a good candidate as a model to

Electronic supplementary material The online version of this article (doi:10.1007/s00214-009-0685-y) contains supplementary material, which is available to authorized users.

F. Wang · D. B. Cao · G. Liu · J. Ren · Y. W. Li (✉)
State Key Laboratory of Coal Conversion,
Institute of Coal Chemistry, Chinese Academy of Sciences,
030001 Taiyuan, China
e-mail: ywl@sxicc.ac.cn

F. Wang · G. Liu
Graduate University of Chinese Academy of Sciences,
100039 Beijing, China

outline the theoretical procedures concerning thermochemical and kinetic calculations of the long-chain alkyl radical reactions. According to the Rice–Kossiakoff radical chain mechanism [2], two different dominating disappearance channels, isomerization and decomposition by β-scission reaction, are available to the 1-C_6H_{13} radical. The former isomerizes by intramolecular hydrogen atom transfer; the latter decomposes by β C–C scission forming a smaller radical and an olefin as shown in Scheme 1. These reactions have been studied experimentally using both steady state and shock-tube techniques [3–9]. 1,5 H atom transfer reaction of 1-hexyl radical was extensively studied by experiment. From the kinetic analysis of the product formation between 298 and 378 K, Watkins [3] obtained the Arrhenius expression for this reaction as $k(T) = 2.57 \times 10^9$ [s^{-1}] $e^{-11.20[kcal/mol]/RT}$. Dóbé et al. [4] generated 1-hexyl in a "bath" of methyl by co-photolysis of 2-octanone with excess acetone or azomethane and obtained $k(T) = 3.16 \times 10^9$ [s^{-1}] $e^{-11.60[kcal/mol]/RT}$ at 300–453 K. Through studying the mechanism and measuring the product rates from hexane pyrolysis at 723–823 K, Imbert et al. [5] indirectly estimated the rate coefficient as $k(T) = 3.16 \times 10^{10}$ [s^{-1}] $e^{-17.02[kcal/mol]/RT}$. Using a shock-tube apparatus coupled with atomic resonance absorption spectrometry, Yamauchi et al. [6] investigated the decomposition and isomerization processes of C_3–C_6 alkyl radicals at 900–1,400 K. The rate coefficient for the 1,5 H atom transfer reaction of 1-hexyl radical was evaluated as $k(T) = 6.65 \times 10^7$ [s^{-1}] $T^{0.82}e^{-12.45[kcal/mol]/RT}$. Available rate coefficients for the decomposition reactions are limited to the reaction of 2-hexyl radical to propylene and 1-propyl radical. On the basis of the kinetics mechanism and the analysis of experimental data in ethane pyrolysis, Quinn [8] gave the rate coefficient with the expression $k(T) = 3.00 \times 10^{13}$ [s^{-1}] $e^{-22.48[kcal/mol]/RT}$ at 800–900 K. Derived from a complex mechanism of ethane pyrolysis at 823–999 K, the high-pressure limit rate coefficient was given by Lin et al. [9] as $k(T) = 3.20 \times 10^{13}$ [s^{-1}] $e^{-26.08[kcal/mol]/RT}$. An estimated rate coefficient with the expression $k(T) = 2.00 \times 10^{13}$ [s^{-1}] $e^{-30.14[kcal/mol]/RT}$ was used by Imbert et al. [5] for modeling hexane pyrolysis at 723–823 K. Recently, significant progress in experimental study of 1-hexyl radical has been made by Tsang et al. [7]. The rate coefficients for the main decomposition and isomerization reactions of 1-hexyl radical were deduced from the product analysis of the shock-tube pyrolysis of 1-hexyl iodide at 890–1,020 K and the Rice–Ramsperger–Kassel–Marcus (RRKM) extrapolation. Unfortunately, most of the rate parameters for the 1-hexyl decomposition and isomerization processes were derived from the analysis of chain reaction systems and often suffered from the hypothesized mechanism model.

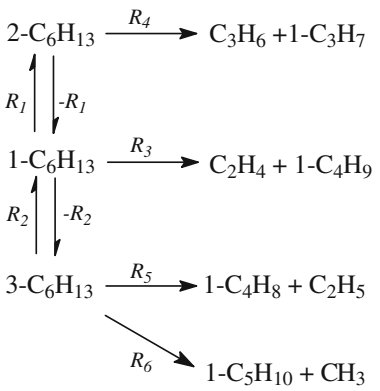

Scheme 1 Primary reaction scheme for disappearance of 1-hexyl radical. (1-C_6H_{13}: 1-hexyl, 2-C_6H_{13}: 2-hexyl, 3-C_6H_{13}: 3-hexyl)

There are a number of theoretical calculations on the decomposition and/or isomerization of alkyl radicals [10–17]. However, there are no theoretical calculations on the rate coefficients of the various possible reactions of 1-hexyl radical, and their branching ratios have not been obtained. Therefore, it is desirable to investigate the mechanism and kinetics of this system by quantum chemical methods. In this paper, we present a systematic study of the competitive decomposition and isomerization channels of 1-hexyl radical using various density functional theory (DFT) methods as well as high-level procedure CBS-QB3 [18]. The aim is to obtain more microscopic insight into the mechanistic and kinetic aspects of the different reactions. The present study includes the calculations on geometries, energies and thermal rate coefficients of the main channels involved. The relative importance of different channels is also discussed in detail. As part of the study, the influence of level of theory on reaction enthalpies and barriers is investigated.

2 Calculation procedures

Electronic structure calculations were performed with the Gaussian 03 program [19]. Unless noted otherwise, calculations on radicals and transition structures were carried out with an unrestricted wave function, as denoted with a "U" prefix. The nature of the located stationary points was characterized according to the number of imaginary vibrational frequencies (NImag = 0 for a minimum or NImag = 1 for a saddle point). The methods used to calculate energy properties include both full optimization and single-point methods; in the latter, denoted X//Y, the energy is calculated at the higher-level X at the geometry obtained by an optimization at the lower level Y. Intrinsic reaction coordinate (IRC) [20] calculations were also carried out to confirm that the transition state structures properly connect reactants and products (see the Supporting Information in Fig. S1).

Geometries of the reactants, products, and transition states were optimized at the MPWB1K [21] and MPW1B95 [21] levels of theory with the 6-31 + G(d,p) basis set as well as the B3LYP/6-311G(2d,d,p) level of theory. In particular, the hybrid meta density functionals MPWB1K and MPW1B95 have been found to give excellent results for thermochemistry and kinetics and to reproduce saddle point geometries well for a large variety of chemical systems [21–23]. We also optimized the geometries at the MPW1B95/6-311 + G(2d,2p) level of theory to show the impact of basis set effect on structures. The calculated geometries at the MPW1B95/6-311 + G(2d,2p) and MPW1B95/6-31 + G(d,p) levels of theory agree with one another fairly well in our study.

Zero-point vibrational energies (ZPVEs) were obtained at the same level of theory as the geometry optimization, and scaled by 0.9537 [21] and 0.9721 [21] for MPWB1K/6-31 + G(d,p) and MPW1B95/6-31 + G(d,p), respectively. As no literature scale factor is available for the MPW1B95/6-311 + G(2d,2p) method, a scale factor of 0.9724 was evaluated by minimizing the root-mean-square errors to reproduce the ZPVEs of the 13 molecules [24]. To yield more reliable reaction enthalpies and barriers, single-point energy calculations were further refined by means of higher-level energy calculations at those methods used in geometry optimization as well as MPW1K [25], BB1K [26], M05-2X [27] and BMK [28]. These new-generated functionals were specifically optimized to give improved performance for studying the kinetics of chemical reactions. The basis set employed for DFT calculations is MG3S which is a very good choice for DFT methods based on its performance and cost [29, 30]. The MG3S basis set is derived from the MG3 basis set by omission of diffuse functions on hydrogens [31]. The single-point energies combined with the ZVPE and thermal corrections obtained from the MPWB1K/6-31 + G(d,p) method were then used for the calculations on the reaction enthalpies and barriers. The CBS-QB3 [32] procedure as a high-level ab initio method was also used. This method is a five-step procedure that starts with the B3LYP/6-311G(2d,d,p) optimized geometry and frequency calculations scaled by a factor of 0.99, followed by energy corrections obtained from CCSD(T), MP4SDQ, and MP2 single-point calculations and a CBS extrapolation. Several studies have already indicated that the CBS-QB3 method offered accurate calculations of thermochemistry and kinetics for hydrogen abstraction [33] and β-scission reactions [34–37]. Therefore, this method was used as a benchmark for comparison.

Thermal rate coefficients of each reaction at the high-pressure limit were computed through the numerical solution to the master equation [38]. This methodology requires a microcanonical rate constant $k(E)$ which can be calculated using the RRKM theory. The basic procedure has been described in detail previously [39] and is not described well here. The isomerization reactions involve hydrogen transfer, and thus the quantum tunneling effect is expected to be noticeable, especially at low temperature. Therefore, the inclusion of these effects was taken into account for these reactions. The one-dimensional Eckart's method [40] was employed to calculate the tunneling coefficient in the rate calculations. The RRKM and master equation calculations were performed using the VKLab program [41] on the basis of the CBS-QB3 energy barriers and the B3LYP/6-311(2d,d,p) frequencies scaled by a factor of 0.99.

3 Results and discussions

3.1 Geometries

The optimized stationary point structures at the MPWB1K/6-31 + G(d,p), MPW1B95/6-31 + G(d,p) and B3LYP/6-311G(2d,d,p) levels of theory along with the MPW1B95/6-311 + G(2d,2p) level of theory are illustrated in Fig. 1 together with their main geometric parameters, while complete geometries in the form of GAUSSIAN archive entries are provided in the Supporting Information. The equilibrium geometries of primary alkyl radicals with a chain carbon skeleton optimized have two conformers; one is that the radical carbon $2p_z$ orbital housing the unpaired electron is eclipsed with a δ C–H bond and the other is that the C $2p_z$ is eclipsed with δ C–C bond. Since the former always has the lower total electronic energy as we obtained, the δ C–H eclipsed radicals were considered in this work.

Examination of Fig. 1 shows that the calculated bond lengths and bond angles in each structure are in good agreement with each other. The average deviation from different level values is generally within 0.02 Å, and the maximum deviation of bond angle is only 0.5°. Furthermore, the calculated structural parameters at the MPWB1K/6-31 + G(d,p) level of theory are slightly closer to those calculated at the levels of MPW1B95/6-311 + G(2d,2p) and MPW1B95/6-31 + G(d,p) than the results obtained from the B3LYP/6-311G(2d,d,p) method. The effect of variation in the theoretical procedure on the bond lengths is generally similar in molecules, radicals and transition states, which has also been noted for decomposition/isomerization reactions [13] and hydrogen abstraction reactions [34, 42].

To assess the effect of the level of theory used for geometry optimization on the computed energies, single-point energy calculations were performed on each structure at the MPWB1K/MG3S level of theory. The resulting reaction barriers and enthalpies without ZPVE corrections

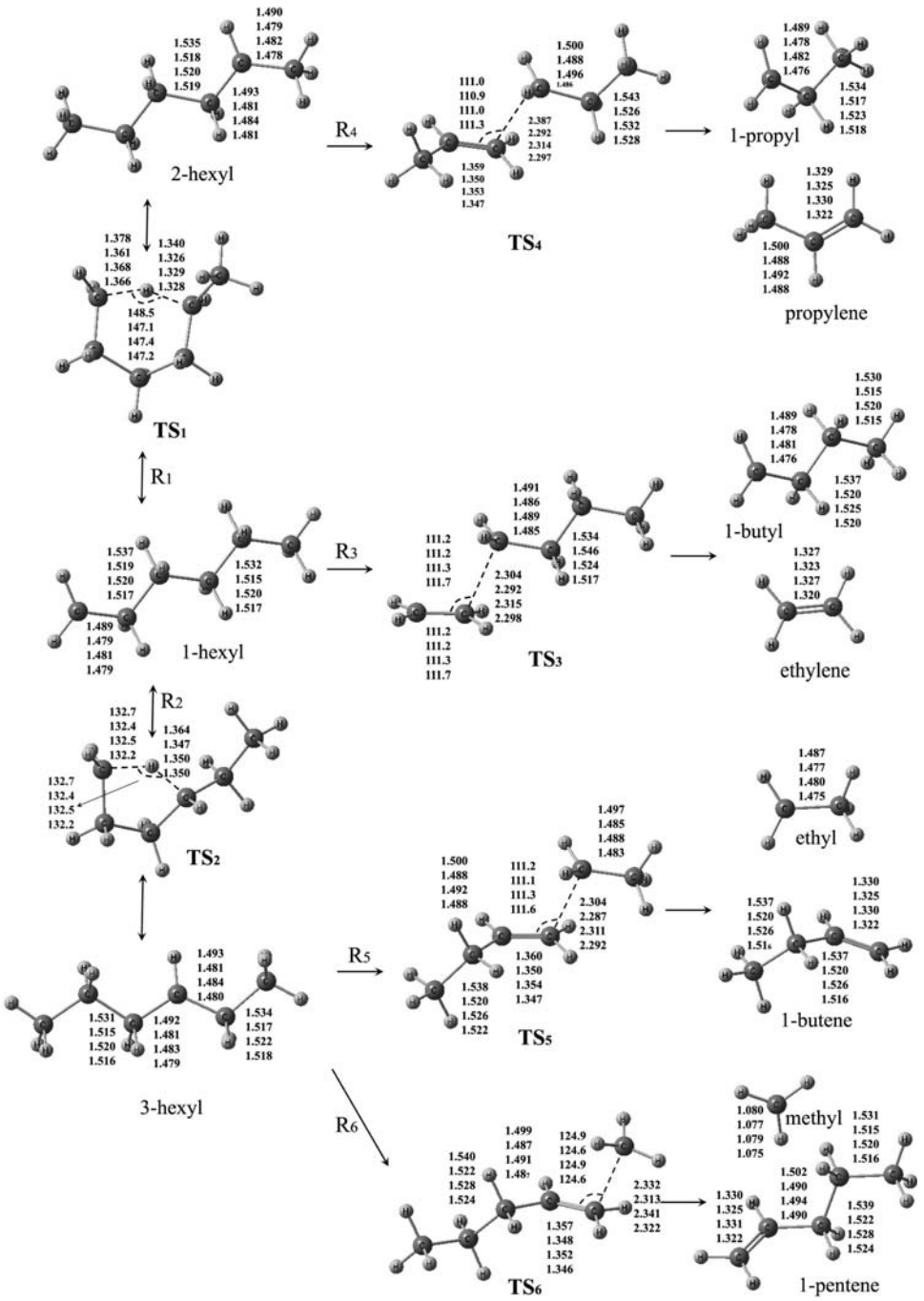

Fig. 1 Optimized geometries for the reactants, products and transition states at several levels. Parameters are given in the order (*top to bottom*): B3LYP/6-311G(2d,d,p), MPWB1K/6-31 + G(d,p), MPW1B95/6-31 + G(d,p) and MPW1B95/6-311 + G(2d,2p) (angle in degrees, distance in Å)

are shown in Tables 1 and 2, respectively. Inspecting the reaction barriers first, we find that the calculated barriers are generally insensitive to the levels of theory used in the geometry optimization. The differences in the barriers are less than or equal to 0.15 kcal/mol. Interestingly, use of the B3LYP/6-311G(2d,d,p) geometries leads to a slight overestimation of the barriers for isomerization reactions and a slight underestimation of the barriers for decomposition reactions in comparison with the corresponding values using other geometries. Examining the reaction enthalpies (Table 2) next, we find that the results are similar to those for the barriers. Once again, the effects of the MPWB1K/6-31 + G(d,p), MPW1B95/6-31 + G(d,p) and MPW1B95/6-311 + G(2d,2p) geometries on the calculated enthalpies are very similar, with deviations of less than 0.31 kcal/mol. Based on the combined results in Tables 1 and 2, the main conclusions are that geometry optimizations are relatively insensitive to the levels of theory used, which means that the reactants, transition state and products are affected similarly by changes in the choice of geometry.

Table 1 Effect of level used for geometry optimization on calculated reaction barriers (kcal/mol)

Level of theory	R_1	R_2	R_3	R_4	R_5	R_6
MPW1B95/6-31 + G(d,p)	17.43	23.74	33.56	34.08	33.56	35.92
MPWBK/6-31 + G(d,p)	17.44	23.74	33.58	34.10	33.58	35.95
MPW1B95/6-311 + G(2d,2p)	17.44	23.75	33.54	34.06	33.54	35.91
B3LYP/6-311G(2d,d,p)	17.55	23.89	33.49	34.02	33.50	35.84

Calculated at the MPWB1K/MG3S level of theory without ZPVEs

Table 2 Effect of level used for geometry optimization on calculated reaction enthalpies (kcal/mol)

Level of theory	R_1	R_2	R_3	R_4	R_5	R_6
MPW1B95/6-31 + G(d,p)	−3.50	−3.38	27.87	27.75	27.90	31.09
MPWB1K/6-31 + G(d,p)	−3.50	−3.37	27.86	27.74	27.89	31.07
MPW1B95/6-311 + G(2d,2p)	−3.51	−3.38	27.80	27.72	27.85	31.03
B3LYP/6-311G(2d,d,p)	−3.57	−3.46	27.56	27.46	27.67	30.89

Calculated at the MPWB1K/MG3S level of theory without ZPVEs

Considering the very close agreements among these results, the MPWB1K/6-31 + G(d,p) geometries were chosen as the base of single-point energy calculations.

In the transition structures (TS_1 and TS_2) corresponding to the isomerization reactions, the distances between the abstracted H atom and the acceptor carbon atom are elongated by 21.54 and 23.35%, respectively, in comparison with the corresponding bonds in the equilibrium structures at the MPWB1K/6-31 + G(d,p) level of theory. The partially formed C–H bonds are longer than the equilibrium values in the stable configurations by 25.09 and 26.39%, respectively, at the same level. Therefore, two transition state structures are early on the potential energy surface, which is consistent with the Hammond's postulate [43]. As shown in Fig. 2, the reactions R_1 and R_2 are exothermic. Closer inspection of the optimized geometries of TS_1 and TS_2 indicates that the partially broken C–H bond and the partially formed C–H bond in five-membered (1,4 transfer) ring transition structure are longer than the corresponding bonds in the six-membered (1,5 transfer) ring transition structure with various methods due to the string strain.

The decomposition of an alkyl radical through a β C–C scission is generally endothermic. Therefore, according to Hammond's postulate [43], the transition state should be late, that is, the saddle point position is close to the product's position along the reaction coordinate. These features were observed in the optimization of the transition state

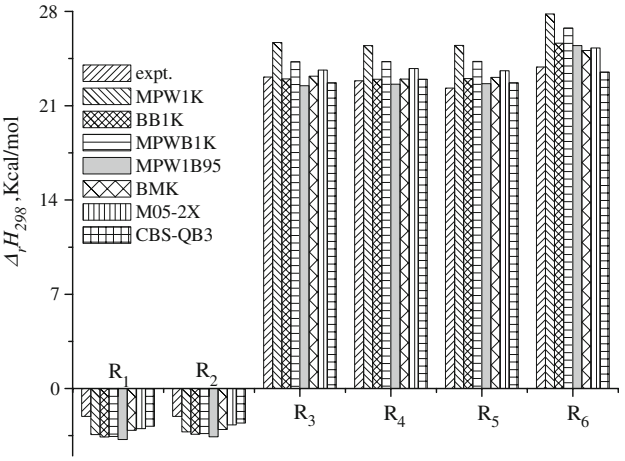

Fig. 2 Calculated reaction enthalpies including ZPVE and thermal corrections with various methods. The DFT calculations using the MG3S basis set on the MPWB1K/6-31 + G(d,p) geometries

structures of the β C–C scission reactions with all the utilized methods. As shown, the transition structures TS_3, TS_4, TS_5 and TS_6 in Fig. 1, the lengths of the partially broken β C–C bonds at the MPWB1K/6-31 + G(d,p) level of theory are longer than the corresponding equilibrium values in normal hexyl radicals by 50.89, 50.99, 50.66 and 52.47%, respectively. When compared with the corresponding bonds in the stationary point structures of olefins, the partially formed C = C bonds in the transition structures, slightly longer by about 1.74–1.89%, represent evidently double bond character. Similarly, the partially formed β C–C bonds in the transition structures have the evident feature of the β C–C bond. From the main geometric parameters of these four structures, it can be found that the saddle point positions on the potential energy surface is close to the product's position, characteristic of endothermic. This trend corresponds to the reaction energy changes as shown in Fig. 2 and Table 4. The relationship between endothermicity of the reactions and their saddle point positions on the potential energy surface was also observed in the MP2/6-311G(d,p) study of 1-pentyl radical decomposition [13].

3.2 Energy properties

The reaction enthalpies ($\Delta_r H_{298}$) including ZVPE and thermal corrections for each reaction were calculated at various levels of theory, using the MPWB1K/6-31 + G(d,p) geometries. The results are shown in Table 3 and Fig. 2. Where possible, the calculated enthalpies were compared with the corresponding gas-phase reference data derived from the standard experimental enthalpies of formation of methyl radical (35.10 ± 0.10 kcal/mol), ethyl radical (28.42 ± 0.31

Table 3 Calculated standard reaction enthalpies relative to reference reaction enthalpies $\Delta_r H°$ (298 K) and MAD (kcal/mol)

		$\Delta_r H$ (calc.) − $\Delta_r H$ (ref.)						
	$\Delta_r H$ (ref.)[a]	MPW1K	BB1K	MPWB1K	MPW1B95	BMK	M05-2X	CBS-QB3
R_1	−2.06	−1.36	−1.55	−1.50	−1.73	−1.04	−0.92	−0.74
R_2	−2.06	−1.16	−1.35	−1.28	−1.52	−0.98	−0.64	−0.50
R_3	23.15	2.57	−0.14	1.14	−0.65	0.05	0.52	−0.42
R_4	22.85	2.62	0.13	1.43	−0.24	0.14	0.91	0.12
R_5	22.31	3.17	0.70	1.98	0.33	0.79	1.28	0.39
R_6	23.87	3.94	1.76	2.90	1.60	1.22	1.41	−0.38
MAD[b]		2.47	0.94	1.70	1.01	0.70	0.95	0.43

In tables, the DFT calculations with the MG3S basis set, using the MPWB1K/6-31 + G(d,p) geometries

[a] The reference values obtained from available experimental enthalpies of formation of the reactants and products as implied by Ref. [42]

[b] Mean absolute deviation

kcal/mol), 1-propyl radical (23.92 ± 0.50 kcal/mol), 1-butyl radical (18.61 ± 0.48 kcal/mol), 1-hexyl radical (8.01 kcal/mol), 2-hexyl radical (5.96 kcal/mol), 3-hexyl radical (5.96 kcal/mol), ethylene (12.54 ± 0.12 kcal/mol), propylene (4.88 kcal/mol), 1-butene (−0.15 ± 0.19 kcal/mol) and 1-pentene (−5.26 ± 2.15 kcal/mol) [44].[1] The reference values have been estimated using the experimental data from a variety of sources. Some of them may be subject to uncertainty, and the comparisons with theoretical values should be viewed in that light. Therefore, the high-level CBS-QB3 results were used to serve as benchmarks for comparison, because it has been demonstrated to provide accurate thermochemistry and kinetics for hydrogen abstraction and β-scission reactions [33–36, 45, 46].

Figure 2 displays the reaction enthalpies at different levels of theory at 298.15 K. In the case of isomerization reactions, the deviations between the CBS-QB3 and M05-2X enthalpies are less than or equal to 0.18 kcal/mol, whereas the MPW1B95 method yields lower values than CBS-QB3 (with a maximum deviation of about 1.02 kcal/mol). For decomposition reactions, the differences between the CBS-QB3 and MPW1B95 enthalpies are smaller than 0.37 kcal/mol with the exception of reaction R_6 for which a larger deviation (1.98 kcal/mol) occurs. However, the differences in the calculated enthalpies at various DFT levels of theory are rather large. The MPW1K method predicts the largest enthalpies and leads to a somewhat larger mean absolute deviation (of 2.03 kcal/mol) from the CBS-QB3 values. The calculated reaction enthalpies are compared to reference values in Table 3. In comparison with the reference reaction enthalpies, the CBS-QB3 method provides better predictions than the DFT methods for each reaction, with a mean absolute deviation of 0.43 kcal/mol, closely followed by the BMK method except for the reaction R_6 for which a larger deviation (1.60 kcal/mol) occurs. The MPW1K method predicts somewhat poorer values with a mean absolute deviation of about 2.47 kcal/mol.

Inspection of the reaction enthalpies resulting from the various methods shows that the isomerization reactions R_1 and R_2 are only two exothermic reactions (ranging from −3.79 to −2.80, and −3.58 to −2.56 kcal/mol, respectively), among the reactions studied. The decomposition processes are thermodynamically unfavorable with large endothermicity, especially the reaction R_6.

Reaction barriers including ZPVE corrections are summarized in Table 4 with different methods, using the MPWB1K/6-31 + G(d,p) geometries, with a view to selecting suitable low-cost procedures for the study of large systems. The CBS-QB3 relative potential energy without ZPVE corrections are shown in Fig. 3. For the isomerizations, the differences in the reaction barriers range from 0.01 to 2.03 kcal/mol, different for different reactions with all the methods except for MPW1B95 which predicts the lowest barriers. The MPWB1K and BB1K barriers are in good agreement with one another (with deviations of less than 0.11 kcal/mol), and consistent with the CBS-QB3 barriers. In the β-scission reactions, the DFT barriers are systematically higher than the corresponding CBS-QB3 values. The MPW1K method provides the maximum values among these methods. The maximum deviation between the MPW1K and CBS-QB3 barriers amounts to 5.96 kcal/mol for the reaction R_6, which are related to the high MPW1K reaction enthalpy (27.82 kcal/mol). The MPW1B95 barriers are similar to the M05-2X values, whereas the BB1K barriers are closer to the BMK values.

[1] Reaction enthalpies $\Delta_r H°(298)$ were calculated as the sum of heat of formation of the products minus those of reactants. The standard enthalpies of formation are from NIST Standard Reference Database (http://webbook.nist.gov) and [44], while the standard enthalpies of formation of 2-hexyl and 3-hexyl radical were derived by assuming the bond dissociation energy of secondary and third C-H bond of *n*-hexane to be 98.09 kcal/mol.

Table 4 Calculated reaction barriers with CBS-QB3 and various DFT methods (kcal/mol)

	Theoretical method						
	MPW1K	BB1K	MPWB1K	MPW1B95	BMK	M05-2X	CBS-QB3
R_1	16.78	15.61	15.62	13.97	16.35	16.55	15.40
$-R_1$	20.31	19.33	19.30	17.87	19.56	19.64	18.26
R_2	23.39	21.78	21.89	20.23	22.65	23.60	22.21
$-R_2$	26.67	25.25	25.29	23.87	25.75	26.36	24.77
R_3	33.59	31.27	31.77	29.32	31.40	29.23	28.36
R_4	33.79	31.64	32.14	29.77	31.64	29.65	28.45
R_5	33.38	31.26	31.73	29.39	31.43	29.24	28.05
R_6	35.05	33.05	33.50	31.37	32.89	30.57	29.09

In tables, the DFT calculations with the MG3S basis set, using the MPWB1K/6-31 + G(d,p) geometries

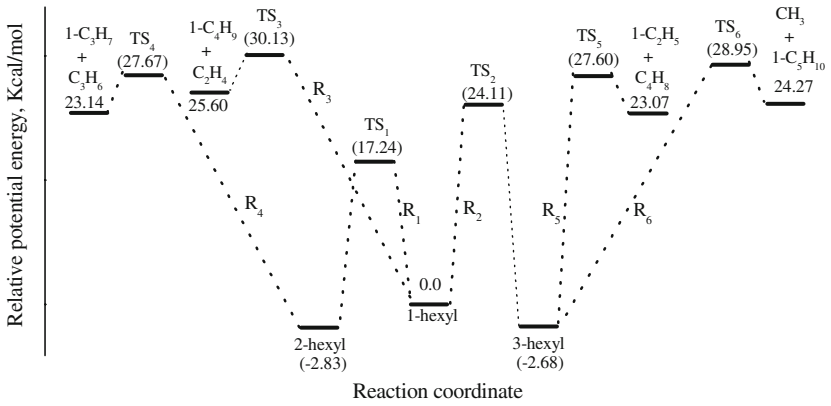

Fig. 3 Total potential energy profiles of considered reactions at the CBS-QB3 level of theory

As shown in Table 4, the isomerization reaction barriers are much smaller than those of the decompositions. This trend is consistent with the previous theoretical calculations [12, 13] and the experimental observations [6, 47]. The smallest reaction barrier is found for the 1,5 H atom transfer reaction R_1 and the largest for the decomposition reaction R_6. A direct comparison of the present results with experiment is difficult, due to the absence of reliable thermodynamic information for the reactions involved in the 1-hexyl system. On the other hand, there have been several theoretical studies of the isomerization of alkyl radicals [13–15]. These reactions (Table 5) are symmetrical or nonsymmetrical processes, but the reaction barriers are expected to provide a source of comparison with the present calculations.

For reaction R_1, our calculations suggest that the reaction barrier is about 15.40–16.78 kcal/mol depending on the method chosen, in good agreement with previous theoretical work on the isomerization reactions involving a six-membered cyclic transition state. We note that a variation of theoretical methods has significant effects on the predicted barriers. Other factors affecting the calculated reaction barriers are in part due to the presence of the substituents and the change of the reaction heat within the same class reaction (the corresponding transition state contains the same number of atoms including H atom in the ring). Generally, the ring in the transition structure carrying substituents causes a decrease of the reaction barriers [14, 17]. For example, the CBS-QB3 reaction barrier of 1,5 isomerization of 1-pentyl radical decreases by about 1.92 kcal/mol when H connected with the partially broken carbon radical is replaced by a methyl group in the six-membered ring of transition state. It is in line with the earlier prediction that the difference of the barrier is about 1.99 kcal/mol at the MP-SAC2 level of theory [14]. In the case of the 1,4 H atom transfer reaction of 1-hexyl radical, it is found to proceed through a barrier of about 20.23–23.60 kcal/mol, which is consistent with the values obtained from the ab initio methods [13, 14].

In the case of decomposition reactions, the calculated barriers of reactions R_3, R_4 and R_5 are quite close to each other, generally within 0.42 kcal/mol, lower than that of the reaction R_6. The computed barriers of the reactions R_4, R_5 and R_6 at the BB1K level of theory are quite close to the earlier values estimated by Tardy et al. [48], generally within 0.44 kcal/mol. On the basis of investigating the addition of hydrogen atom to trans-3-hexene at 573 K and low pressure, they estimated that the barriers for the reactions R_4, R_5 and R_6 are 31.20, 31.25 and 33.15 kcal/mol, respectively. These values are higher than the corresponding MPW1B95 barriers by about 1.43–1.86 kcal/mol.

Table 5 Comparison of the theoretical reaction barriers including ZPVEs for isomerization reactions in normal and branched radicals (kcal/mol)

Type of process	Reaction	
	1,4	1,5
Thermoneutral (*n*-alkyl radical)[a]	24.60	17.20
Thermoneutral (*n*-alkyl radical)[a]	25.10	18.80
Thermoneutral (1-butyl radical)[b]	24.80	18.76
Thermoneutral (1-alkyl radical)[c]	25.26	14.20
Exothermic (1-pentyl radical)[d]	19.10	13.43
Exothermic(2-methyl-hex-1-yl)[e]	20.59	14.60
Exothermic(*n*-alkyl radical)[f]	21.50	16.58
Exothermic(1-hexyl radical)[c]	23.13	

[a] MP-SAC2//UHF/6-31G(d) and BAC-MP4 results in Ref. [15]

[b] CCSD(T)/cc-pVDZ//BH&HLYP/cc-pVDZ result in Ref. [16]

[c] G3MP2B3 results in Ref. [17]

[d] MP-SAC2/6-311G(d,p) in Ref. [13]

[e] MP-SAC2//MP2/6-311G(d,p) results in Ref. [14]

[f] results from an RRKM analysis of the experimental results and the previous lower temperature data in Ref. [6]

In the 1-hexyl system, as expected, the reaction R_1 with exothermicity proceeds via a transition state TS_1 with the lowest reaction barrier. With a higher ring strain, the reaction barrier of the reaction R_2 increases about 6.17–7.05 kcal/mol in comparison with that of reaction R_1 depending on the methods used. Similarly, for their reverse reactions ($-R_1$ and $-R_2$), the process with a larger ring of transition state has a lower barrier. They, however, are endothermic with higher reaction barriers than the corresponding reverse processes. Inspection of the data obtained (Fig. 2; Table 3) shows that the decomposition processes considered are thermodynamically unfavorable with large endothermicity. The theoretical results suggest that these channels are different in their TS structures depending on the different environments of the C–C bond in the reactant conformations. This difference implies their different contributions to the whole system. In the calculations of rate coefficients, we have shown different behaviors of these channels which are due to their barriers and the position of C–C scissions.

If we examine isomerizations and decompositions as independent problems, the results are more encouraging. For the isomerization reactions, methods such as BB1K and MPWB1K, which produces enthalpies within 0.85 kcal/mol of the CBS-QB3 values and barriers within 1.05 kcal/mol, would be suitable for large systems. For the decompositions, the MPW1B95 or M05-2X methods appear to be suitable, both producing enthalpies within 0.94 kcal/mol of the CBS-QB3 values and barriers within 1.34 kcal/mol with the exception of reaction R_6.

3.3 Rate coefficients and branching ratios

To estimate the relative importance of the different reaction channels, we calculated the thermal rate coefficients by using the master equation [38] in a temperature range of 250–2,500 K at the CBS-QB3 level of theory. The results together with the data by experiment and theory in literature are shown in Fig. 4. It could be found that the tunneling effect is more crucial for H atom transfer reactions than for decompositions in the low-temperature area.

For the 1,5 H atom transfer reaction of 1-hexyl (R_1), we note that the available rate coefficients were obtained over various temperature intervals. However, when two studies covering approximately the overlapping temperature range 500–1,300 K (see Yamauchi et al. [6] and Tsang et al. [7]) are compared with our results, we show that the CBS-QB3 rate coefficient is covered by experiment. However, our values are higher than that from Yamauchi et al. [6] and Tsang et al. [7] within a factor of 3.11 or less at 500–1,300 K. In the lower temperature range (lees than 350 K), however, no experimental data are available to compare with the computed data for this reaction. The rate coefficient of the reaction R_4 has been reported by Quinn [8], Lin et al. [9] and Imbert et al. [5], respectively. Large discrepancies exist among the obtained rate coefficients, with respective activation energies of 22.48, 26.08 and 30.14 kcal/mol and preexponential factors of 3.02×10^{13}, 3.16×10^{13} and 2.00×10^{13} s^{-1}, respectively. If we compare the calculated rate coefficient of this reaction with that of Imbert et al. [5], the difference is within a factor of 2.50 at 723–823 K. It is noteworthy that our theoretical rate coefficients are in good agreement with the values of Tsang et al. [7] in all cases. Therefore, the CBS-QB3 rate coefficients with the Eckart approximation are reasonable for describing the reaction processes of the studied system. The individual rate coefficients were fitted by least squares to the following Arrhenius expressions in s^{-1} at 250–2,500 K:

$$k_1(T) = 1.52 \times 10^8 (T/298)^{3.11} e^{-8.94/RT}$$

$$k_{-1}(T) = 5.56 \times 10^7 (T/298)^{3.36} e^{-10.58/RT}$$

$$k_2(T) = 4.58 \times 10^6 (T/298)^{5.02} e^{-11.91/RT}$$

$$k_{-2}(T) = 1.31 \times 10^6 (T/298)^{5.10} e^{-14.50/RT}$$

$$k_3(T) = 7.32 \times 10^{13} (T/298)^{0.64} e^{-29.66/RT}$$

$$k_4(T) = 2.37 \times 10^{13} (T/298)^{0.69} e^{-29.88/RT}$$

$$k_5(T) = 1.69 \times 10^{13} (T/298)^{0.70} e^{-29.53/RT}$$

$$k_6(T) = 1.39 \times 10^{13} (T/298)^{0.88} e^{-30.56/RT}$$

The rate calculations allow us to estimate the relative importance of the different channels. The CBS-QB3 branching ratios of each reaction channel as a function of

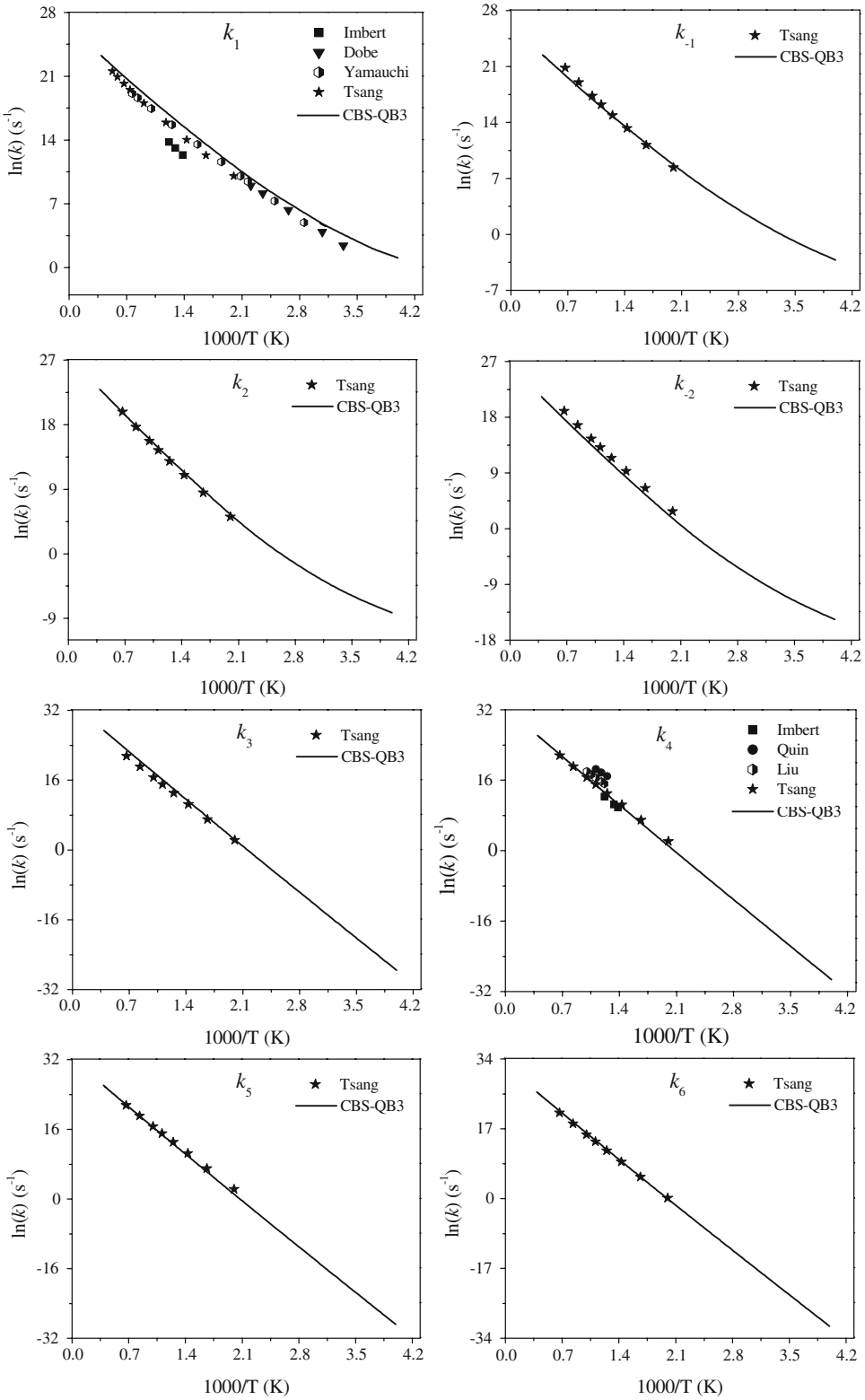

Fig. 4 Arrhenius plot of rate coefficients calculated at the CBS-QB3 level of theory together with the experimental data from Ref. [4–7]. *Symbols* the data by experiment and theory in literature; *solid lines* our theoretical results

temperature are shown in Fig. 5. The branching ratio ρ is defined as the ratio of the rate coefficient k_i of a channel to the sum of those for all channels ($\rho = k_i/\sum k_i$).

As discussed above, the large difference in the reaction barriers indicates that the relative importance of the various channels is significantly different. For the isomerization

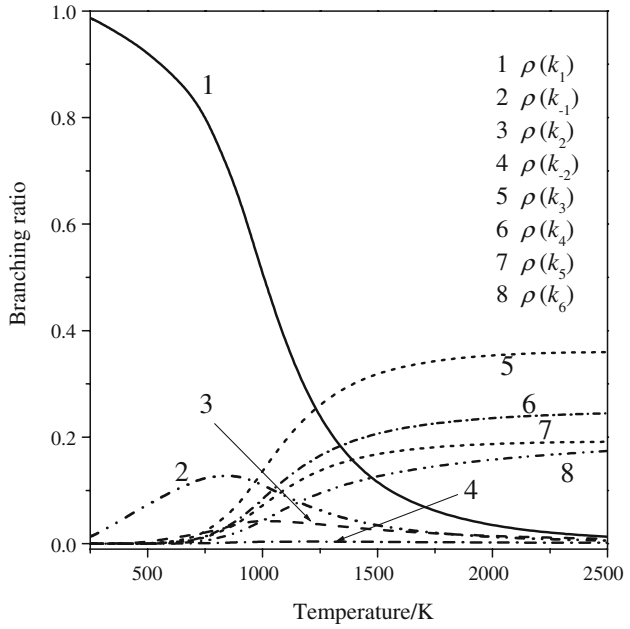

Fig. 5 Calculated branching ratios of considered reactions in the 1-hexyl system at different temperatures with the CBS-QB3 method ($\rho = k_i/\sum k_i$)

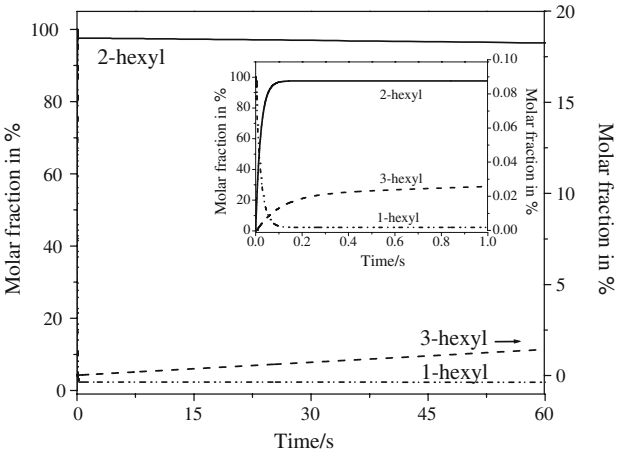

Fig. 6 Distributions of normal hexyl radicals as a function of reaction time at 300 K and 101.3 kPa. The 3-hexyl curve corresponds to the right axis

processes, the largest rate coefficient characterizes the 1,5 H atom transfer reaction (R_1) which also has the lowest barrier. However, with an increase of temperature, its branching ratio to the sum of the isomerization channels decreases. But it is still a major channel of the isomerizations in the whole temperature range considered as it is the most exothermic channel with the lowest barrier. Therefore, under both thermodynamically and kinetically controlled conditions, i.e., at high and low temperatures, the 1-hexyl→2-hexyl isomerization process involving a six-membered cyclic transition state is the more favorable channel. This is consistent with the calculated branching ratios with temperatures observed (Fig. 5). The following important isomerization is the reaction $-R_1$. With an increase in temperature, the branching ratio of the reaction $-R_1$ passed through a maximum, and the maximum branching ratio is about 0.13 at 800 K. For the isomerization reactions R_2 and $-R_2$, their contributions to the whole system are not significant, less than 0.05 in the whole temperature range. This means that these two reactions can be negligible under normal pyrolysis conditions.

Competing with the isomerization reactions is the decomposition reactions via splitting a β C–C bond to produce an olefin and a small alkyl radical. The importance of the reaction via β C–C scission is the reaction R_3 which is the fastest channel among the decomposition processes. At 250 K, this reaction is responsible for over 48.14% of the decomposition reactions, while at high temperature this fraction somewhat decreases, but still plays an important role. The second most significant channel is the reaction R_4 producing propylene and 1-propyl radical. Its contribution to the total rate become more and more important and amounts to about 24.48% at 2,500 K. Though the decomposition reaction R_6 is the thermodynamically least favored reaction among the processes studied, the CBS-QB3 results indicate that, under normal pyrolysis conditions, even the R_6 may gain some importance (its branching ratio is about 0.09 at 1,200 K).

Figure 6 shows the trend of the normal hexyl radical distributions from the 1-hexyl disappearance plotted against the time at 300 K and 101.3 kPa. It clearly validates that there is an equilibrium process involving the isomeric forms of the normal hexyl radicals at relative low temperature because the isomerization of a long-chain radical gets across a lesser barrier than its decomposition. Moreover, the state of quasiequilibrium for the faster isomerization processes is nearly unaffected by the decomposition processes. However, under high-temperature conditions, this equilibrium is demolished for the contribution of the decomposition reactions to the whole system increases. For example, the decomposition of 1-hexyl radical to ethylene and 1-butyl radical (R_3) dominates over the reaction R_1 and become primary. The branching ratio of this reaction is responsible for over 0.25, higher than the reaction R_1 at 1,200 K.

The CBS-QB3 results suggest that the isomerization reactions are dominating and responsible for over 82.17% of all the reactions in the low-temperature range 300–900 K. However, direct decomposition processes compete favorably with the isomerization processes under higher-temperature conditions. It indicates that the Rice–Kossiakoff mechanism [2] (isomerization reaction rates ≫ decomposition reaction rates) becomes more reasonable with the

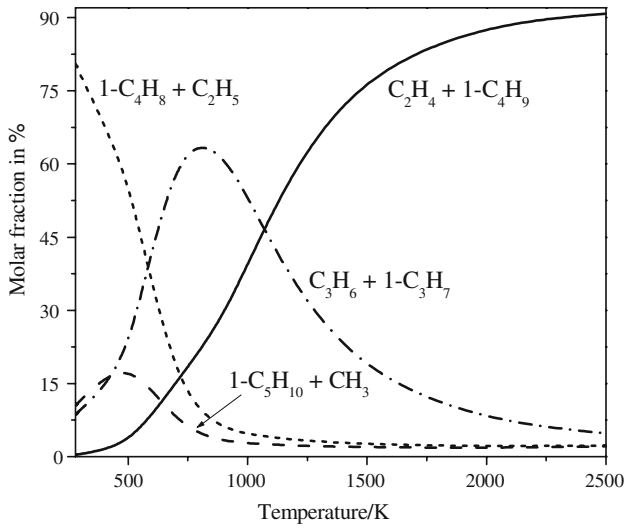

Fig. 7 Product distributions from 1-hexyl radical decomposition as a function of reaction temperature at 101.3 kPa

decrease of temperature, while in more usual pyrolysis conditions both classes of reactions are kinetically competitive and simultaneously important.

The temperature effect on the product distributions from 1-hexyl radical is illustrated in Fig. 7. As shown in Fig. 7, temperature changes have a significant effect on the distribution of the products. The further analysis suggests that an increase in temperature results in an increase in the branching ratio of decomposition/isomerization reactions. Higher temperature, that is, favors the unimolecular decomposition of alkyl radicals against the isomerization process, consistent with experimental observations in hydrocarbon pyrolysis [1]. The rate balance of these reactions will further determine the actual propagation steps that occur and therefore the selectivity among the products that are formed.

4 Conclusions

In this work, we have investigated decomposition and isomerization processes of a model system involved in hydrocarbon pyrolysis, namely, the 1-hexyl system with various computational methods. The following conclusions may be drawn.

(1) Optimized geometries are relatively insensitive to the levels of theory used, and their variation has a slight effect on the calculated reaction enthalpies and barriers. However, the theoretical methods affect significantly reaction enthalpies and barriers on a given structure. The best agreement with the reference reaction enthalpies for each reaction is obtained by the CBS-QB3 method. Moreover, thermal rate coefficients predicted by this method are covered by experimental data fairly well. As alternative methods, the BB1K/MG3S//MPWB1K/6-31 + G(d,p) and MPWB1K/MG3S//MPWB1K/6-31 + G(d,p) methods are slightly superior to other DFT methods for the isomerization reactions of long-chain alkyl radicals, whereas the MPW1B95/MG3S//MPWB1K/6-31 + G(d,p) and M05-2X/MG3S//MPWB1K/6-31 + G(d,p) methods appear to be suitable for the decomposition reactions of the alkyl radical system with six carbons or more.

(2) As expected, the reaction barriers for 1,5 H atom transfer reactions are lower than those for 1,4 H atom transfer reactions by about 5.91–7.05 kcal/mol depending the method used. The decomposition processes studied are thermodynamically unfavorable with large endothermicity. This difference implies their relative importance in the 1-hexyl system.

(3) Under the conditions considered, the temperature effect is shown to be important especially in the branching ratios for higher barrier reactions such as β C–C scissions in competition with isomerization reactions. At low temperatures, isomerization processes involving a five- and six-membered cyclic transition state are completely dominating, while β C–C scission reactions are shown to compete favorably with them under high-temperature conditions (up to 1,000 K). The results make clear that the equilibrium process involving the isomeric forms of normal hexyl radicals at relative low temperature is demolished under higher-temperature conditions because the contribution of the decomposition reactions to the whole system increases.

Acknowledgments The authors gratefully acknowledge the financial support from National Natural Science Foundation of China under Grant No. 20590361 and the National Outstanding Young Scientists Foundation of China under Grant No. 20625620. This work is also supported by Synfuels China Co., Ltd.

References

1. Albright LF, Crynes BL, Corcoran WH (eds) (1983) Pyrolysis: theory and industrial practice. Academic Press, New York
2. Kossiakoff A, Rice FO (1943) J Am Chem Soc 65:590
3. Watkins KW (1973) J Phys Chem 77:2938
4. Dóbé S, Bérces T, Réti F, Márta F (1987) Int J Chem Kinet 19:895
5. Imbert FE, Marshall RM (1987) Int J Chem Kinet 19:81
6. Yamauchi N, Miyoshi A, Kosaka K, Mitsuo K, Matsui H (1999) J Phys Chem A 103:2723
7. Tsang W, Walker JA, Manion JA (2007) Proc Combust Inst 31:141
8. Quinn CP (1963) J Chem Soc Faraday Trans 59:2543
9. Lin MC, Back MH (1966) Can J Chem 59:2369
10. Chen YH, Rauk A, Tschuikow-Roux E (1990) J Phys Chem 94:6250
11. Pacansky J, Waltman RJ, Barnes L (1993) J Phys Chem 97:10694

12. Jitariu LC, Wang H, Hillier IH, Pilling MJ (2001) Phys Chem Chem Phys 3:2459
13. Jitariu LC, Jones LD, Robertson SH, Pilling MJ, Hillier IH (2003) J Phys Chem A 107:8607
14. Viskolcz B, Lendvay G, Seres L (1997) J Phys Chem A 101:7119
15. Viskolcz B, Lendvay G, Kortvelyesi T, Seres L (1996) J Am Chem Soc 118:3006
16. Bankiewicz B, Huynh LK, Ratkiewicz A, Truong TN (2009) J Phys Chem A 113:1564
17. Hayes CJ, Burgess DR Jr (2009) J Phys Chem A 113:2473
18. Montgomery JA, Frisch MJ, Ochterski JW, Petersson GA (1999) J Chem Phys 110:2822
19. Frisch MJ, Pople JA et al (2004) Gaussian 03, Revision E.01. Gaussian Inc., Wallingford, CT
20. Gonzalez C, Schlegel HB (1989) J Chem Phys 90:2154
21. Zhao Y, Truhlar DG (2004) J Phys Chem A 108:6908
22. Zhao Y, Truhlar DG (2005) J Phys Chem A 109:5656
23. Albu TV, Swaminathan S (2006) J Phys Chem A 110:7663
24. Fast PL, Corchado J, Sanchez ML, Truhlar DG (1999) J Phys Chem A 103:3139
25. Lynch BJ, Fast PL, Harris M, Truhlar DG (2000) J Phys Chem A 104:4811
26. Hamprecht FA, Cohen AJ, Tozer DJ, Handy NC (1998) J Chem Phys 109:6264
27. Zhao Y, Schultz NE, Truhlar DG (2006) J Chem Theory Comput 2:364
28. Boese AD, Martin JML (2004) J Chem Phys 121:3405
29. Zhao Y, Lynch BJ, Truhlar DG (2005) Phys Chem Chem Phys 7:43
30. Zheng JJ, Zhao Y, Truhlar DG (2007) J Chem Theory Comput 3:569
31. Lynch BJ, Zhao Y, Truhlar DG (2003) J Phys Chem A 107:1384
32. Montgomery JA, Frisch MJ, Ochterski JW, Petersson GA (2000) J Chem Phys 112:6532
33. Vandeputte AG, Sabbe MK, Reyniers MF, Van Speybroeck V, Waroquier M, Marin GB (2007) J Phys Chem A 111:11771
34. Coote ML (2004) J Phys Chem A 108:3865
35. Sabbe MK, Vandeputte AG, Reyniers MF, Van Speybroeck V, Waroquier M, Marin GB (2007) J Phys Chem A 111:8416
36. Saeys M, Reyniers MF, Marin GB, Van Speybroeck V, Waroquier M (2003) J Phys Chem A 107:9147
37. Iuga C, Galano A, Vivier-Bunge A (2008) ChemPhysChem 9:1453
38. Gilbert RG, Smith SC (eds) (1990) Theory of unimolecular and recombination reactions. Blackwell Scientific Publications, Oxford
39. Miller JA, Klippenstein SJ (2006) J Phys Chem A 110:10528
40. Eckart C (1930) Phys Rev 35:1303
41. Zhang S, Troung TN (2001) VKLab. Version 1.0, University of Utah
42. Hemelsoet K, Moran D, Van Speybroeck V, Waroquier M, Radom L (2006) J Phys Chem A 110:8942
43. Hammond GS (1955) J Am Chem Soc 77:334
44. Lide DR (2006) CRC Handbook of chemistry and physics, 87th edn. CRC Press, Boca Raton, FL
45. Zheng XB, Blowers P (2007) Theor Chem Acc 117:207
46. Gomez-Balderas R, Coote ML, Henry DJ, Radom L (2004) J Phys Chem A 108:2874
47. Ross PL, Johnston MV (1995) J Phys Chem 99:16507
48. Tardy DC, Rabinovitch BS, Larson CW (1966) J Chem Phys 45:1163